

Random sample consensus-based room mapping using light detection and ranging

Merlyn Inova Christie Latukolan¹, Aloysius Adya Pramudita¹, Nasrullah Armi^{1,2}, Nizar Alam Hamdani³, Helfy Susilawati³, Arief Suryadi Satyawan^{2,4}

¹Department of The CoE Intelligent Sensing-IoT, Telkom University, Bandung, Indonesia

²National Research and Innovation Agency (BRIN), Research Center for Telecommunication, Bandung, Indonesia

³Department of Electrical Engineering, Universitas Garut, Garut, Indonesia

⁴Faculty of Engineering, Nurtanio University, Bandung, Indonesia

Article Info

Article history:

Received Jun 9, 2023

Revised Aug 13, 2024

Accepted Aug 25, 2024

Keywords:

Light detection and ranging

Line-fitting

Point cloud

RANSAC

Room mapping

ABSTRACT

Light detection and ranging (LiDAR) is a high-accuracy data source for geospatial providers that is displayed in two dimensions (2D) or three dimensions (3D). It is used to measure the distances or 2D or 3D maps of the environment. This study examines a random sample consensus (RANSAC)-based room mapping approach utilizing LiDAR. The RANSAC is used to achieve line fitting as a solution to acquire missing or incomplete point cloud data during the process of room scanning. The maximum x-y distance is proposed to achieve a proper model to fix the missing line during the LiDAR scanning process. Data retrieval uses ground-based LiDAR located in the middle of a certain room with the dimension of 5.76×4.95 m². To explore a room mapping, a 2D LiDAR YDLIDAR G4 with an operating frequency of 7 Hz is used. The derived raw data is then visualized with MATLAB. The results show that the RANSAC can perform line-fitting for missing or illegible LiDAR point cloud data during the scanning process due to reflection or obstacles. The increase in the amount of data used is then directly proportional to the probability of the number of correct models.

This is an open access article under the [CC BY-SA](https://creativecommons.org/licenses/by-sa/4.0/) license.



Corresponding Author:

Nasrullah Armi

National Research and Innovation Agency (BRIN), Research Center for Telecommunication

Sangkuriang Dago Road, Bandung, Indonesia

Email: nasr004@brin.go.id

1. INTRODUCTION

Recently, the need for geospatial information has increased. Geospatial information relates to geographical location, spatial dimension and the characteristics of natural objects. In addition, geospatial information plays an important role in remote sensing technologies such as spatial planning, mapping (i.e., forest, land, and urban planning), disaster mitigation and assistance tools for autonomous vehicles. Light detection and ranging (LiDAR) is one technology for remote sensing applications. It offers high precision geospatial data and displays in the form of 2D or 3D dimensions. LiDAR can be mounted on the ground, airborne, space borne, or submarine [1]-[7].

While geospatial data is obtained with high precision, during the scanning process, LiDAR is often miss-detected. This definitely leads to an error in object or space visualization. Water as a non-reflected object, glass as an object with imperfect reflection, and object position with a LiDAR signal out of range are some causes of LiDAR miss-detection. A space with a lot of glass barriers can definitely not be well mapped.

In previous works, some methods have been proposed to optimize the processing of LiDAR data. Region Growth, 3D Hough Transform, and random sample consensus (RANSAC) are the 3 popular LiDAR

data processing methods. However, Tarsha-Kurdi *et al.* [8] claim that RANSAC is more efficient in the case of LiDAR point cloud processing time and sensitivity. The RANSAC is then used for LiDAR applications [9]-[12].

LiDAR based area mapping was studied [13]-[20]. Using object-based image analysis and the support vector machine, mapping on a mangrove forest using LiDAR data was investigated in [21], [22]. Currently, LiDAR is used for autonomous vehicle applications [23]-[28]. The use of LiDAR benefits to avoid obstacles and navigation for driving. LiDAR is used for real-time detection of road boundaries as well. It is critical for autonomous vehicle applications such as vehicle localization, path planning, and environmental understanding. By embedding LiDAR sensors in autonomous vehicles, it is possible to build multi-object tracking.

Regarding the above-mentioned literature surveys, the RANSAC works primarily on airborne LiDAR. However, the RANSAC is also used to segment building roof planes. The used method for detection is affected by local structures such as trees and antennas. The RANSAC based detection algorithm was proposed in [29]. The proposed algorithm with 2D LiDAR data was used to detect road edge under structured and semi-structured road environment. Furthermore, Satyawan *et al.* [30] introduced the RANSAC for estimating room mapping using point cloud 2D. However, it excludes the achieved outlier data and only uses inlier data to estimate a room. This paper investigates the RANSAC for estimating room mapping and shape using outlier data. This information is used to replace the missing line. This paper is divided into four sections. The first section provides background information and related works, followed by a description of the work contribution. The second section describes the method and experiment. The third section discusses the outcome and the process of compiling the room mapping. Finally, in the fourth section, the work is concluded.

2. METHOD

This section discusses the LiDAR experiment and the data processing software. The computer specification used is AMD A10-9600P Radeon R5, 10 Computer Cores 4 C+6 G 2.40 GHz, 8 GB of RAM with MATLAB R2018b installed. The diagram block for the experiment is described in Figure 1. It is constructed by LiDAR equipment for the scanning process and computing equipment as a data processing tool. The speed of LiDAR rotation is affected by the setup of the frequency. By using MATLAB as data processing tool, distance and elevation data are converted into x and y coordinates. This converted data is then visualized in a room map. The RANSAC method is applied to reconstruct the missing detected object using line fitting.

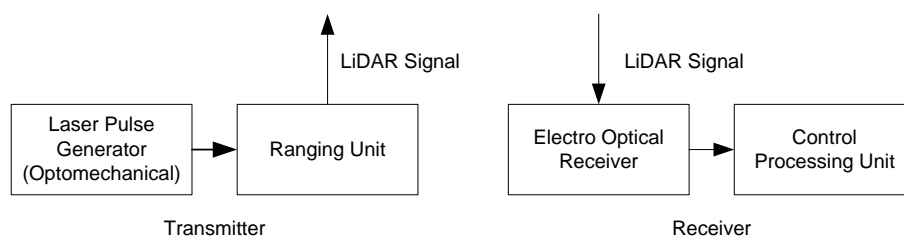


Figure 1. LiDAR block diagram

As mentioned in the YDLIDAR G4 2D specification, the frequency of the LiDAR motor used is 7 Hz. This frequency must be adjusted prior to the scanning process. When the data is derived during the scanning process, the software converts the data into x and y coordinates and the calculation (1) and (2):

$$x = d \times \cos(\theta_{rad}) \quad (1)$$

$$y = d \times \sin(\theta_{rad}) \quad (2)$$

then, the processing tool visualizes the converted data and optimize it using RANSAC method.

LiDAR block diagram has transmitter and receiver. The transmitter generates laser pulse to shoot into objects. When the objects reflect the pulse, receiver calculates travel time to derive the distance between objects and LiDAR. The experiment is conducted in a room with a dimension of less than 16 m². In

comparison, we measure the room manually. LiDAR is located in the middle of the room, as shown in Figure 2.

LiDAR is connected to a USB Type-C or PH2.0-5P PC as an interface slot. To activate LiDAR communication, one slot must be selected. USB Type-C is used for data communication and power systems. The PH2.0-5P slot is used for power supply and data communication.

LiDAR rotates 3,600 automatically and hits objects (obstacles) inside a room. The derived data are distance (mm) and angle reference (degree). The data is converted into a co-ordinate and processed by MATLAB using the RANSAC method to obtain a 2D room map. Visualization of LiDAR data is performed twice, using angle data with the degree unit and data with radian converted. The radian converted data is then divided into 4 groups based on x and y axis.

The experiment is carried out in two steps, using developed and undeveloped methods. The results of undeveloped method is used as reference for improvement. The process of grouping data as a part of LiDAR data processing is conducted twice. First, grouping based on x and y axis location as main data group. Then, grouping based on median of main data group. Grouping based on median is used due to its less sensitivity to the presence of outlier. This reason fits to the characteristics of RANSAC method. Grouping data based on median is conducted repeatedly until the data requirements fulfilled.

This experiment uses MATLAB as a tool to process the data. The RANSAC method is implemented after the LiDAR data has been visualized. The number of samples is determined prior to implementation. This experiment takes two samples that meets the minimum requirements to form a line. If a number of data is less than the number of samples, the method cannot be used. If the number of data matches and exceeds the sample size, two data is selected randomly. Then, the number of outliers and inliers is calculated. If the number of inliers exceeds the specified threshold, the identified inliers is then used to create a new model, while the outliers is ignored. If it does not exceed the threshold, the random selection of two pieces of data is then repeated by taking into account the number of iterations. If the maximum number of iterations is 1,000, the RANSAC method is no longer used.

Furthermore, the parameters used in this experiment are as follows:

- Angle: the angle data used in this experiment is the result of reading LiDAR data in degrees. This angular data is converted into radians which is used to calculate the x and y coordinates.
- Distance: the distance data used is the result of LiDAR readings in millimetres. The distance data is combined with the angle data to determine the x and y coordinates.
- Median: the median is used to divide the main group into smaller groups. This is taken to improve the RANSAC method's results.
- Number of samples: since these samples are used for line-fitting, the total number of samples used in this experiment is two from the total results. The RANSAC method in MATLAB allows for a maximum of 100 samples to be used.
- Maximum distance: this parameter is related to the threshold used to identify outliers and determine whether data falls into the inlier category. After repeating the experiment several times, the value of this parameter can be adjusted, and the minimum value is 2. It should be noted that increasing the value of this parameter speeds up the algorithm but reduces the accuracy of the results.
- Probability: in this experiment, the probability that the selected sample is 99% inlier according to the default in MATLAB. With high probability, the algorithm is most likely more stable, but the processing time becomes longer.

We use the RANSAC method to reconstruct missing point cloud data during the LiDAR scanning process by line-fitting the room map generated after processing LiDAR. Line-fitting is expected to project the missing room edge data with a line. LiDAR is in a static position and is placed in the middle of a 5.76×4.95 m² room to retrieve data. Figure 3(a) shows data retrieval using a YDLIDAR G4 with a motor frequency of 7 Hz. The room where the data is collected is not empty, and there are several objects that is able to alter the room's original shape. Figure 3(b) shows the area of the room affected by LiDAR scanning, where x represents the position of the LiDAR in the center of the room and the red line represents the area of the room exposed to the scanning. The number of data obtained is 1,773 for a single retrieval. Figure 4 shows LiDAR data.

After the data is collected, it is plotted to visualize the shape of the room by exploiting original angle and distance data. Then, the plotting results is analyzed to determine the location or position as well as the number of line-fittings required. The data is divided into several groups prior to implementing the method. The data is processed with two steps using the RANSAC method. The first step is undeveloped method, while the second step is developed method.

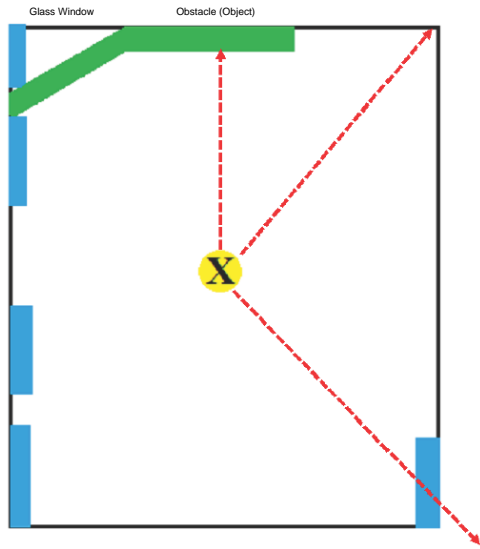


Figure 2. Experiment space for data retrieval



(a) (b)

Figure 3. Experiment of room mapping using LiDAR; (a) YDLIDAR G4 and (b) a room for data retrieval

	A	B	C	D	E	F
1	Original Angle	Correction Value	Correction Angle	Zero Angle	Distance	Quality
2	348.109375	-7.515625	340.59375	0	2651	252
3	348.34375	-7.515625	340.828125	0	2657	252
4	348.625	-7.515625	341.109375	0	2657	252
5	348.90625	-7.515625	341.390625	0	2659	252
6	349.1875	-7.515625	341.671875	0	2663	252
7	349.46875	-7.515625	341.953125	0	2663	252
8	349.75	-7.515625	342.234375	0	2664	252
9	350.03125	-7.53125	342.5	0	2669	252
10	350.328125	-7.515625	342.8125	0	2668	252

Figure 4. LiDAR data

3. RESULTS AND DISCUSSION

LiDAR data is visualized by plotting the x and y points obtained by solving (1) and (2). The visualization results shown in Figure 5 which are taken from YDLIDAR G4 software. Figure 6(a) shows the visualization of LiDAR data with MATLAB by calculating the x and y points using angle data in degrees and distances. In Figure 6(b), LiDAR data is visualized by calculating the x and y points using angle data that is converted into radians and distances. The RANSAC method is used to reconstruct the missing parts of the room map using line-fitting.

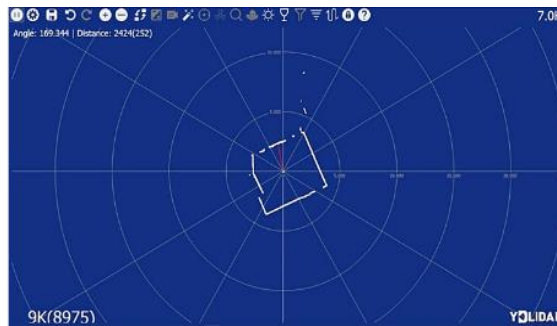
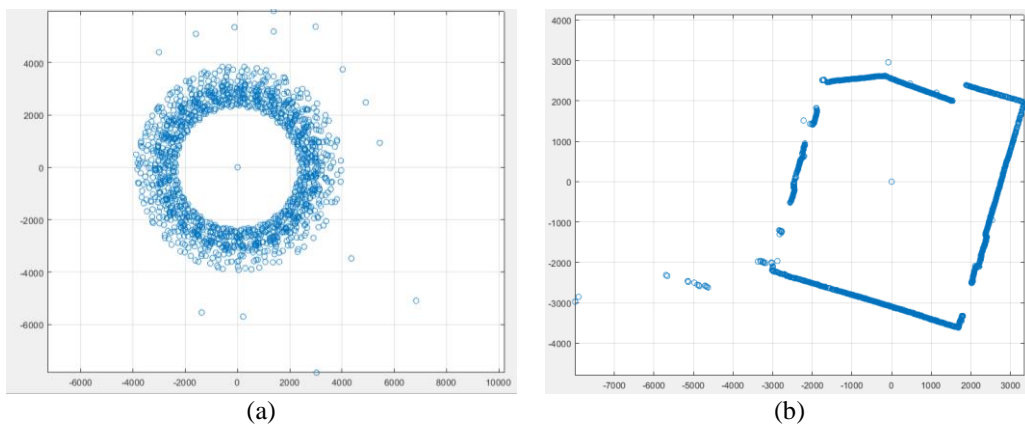


Figure 5. Visualization of LiDAR data using YDLIDAR software



(a) (b)

Figure 6. Visualization of LiDAR data with x and y axes show the distance between detected points and LiDAR position in mm; (a) in degree unit and (b) in radian unit

Data grouping is performed to reconstruct missing data on the room map with line-fitting. The results is illustrated in Figure 7. Label A shows the results without ignoring the point (0,0), whereas label B shows the results with ignoring the point (0,0). The point (0,0) in Figure 7(a) affects identification process for RANSAC's inlier. RANSAC is able to identify the inlier in Figure 7(b), but the line-fitting position is insufficient. Based on the results, it is concluded that the results with ignoring the point (0,0) in Figure 7(b) are closer to the expected result than Figure 7(a). Hence, data is grouped by ignoring the point (0,0).

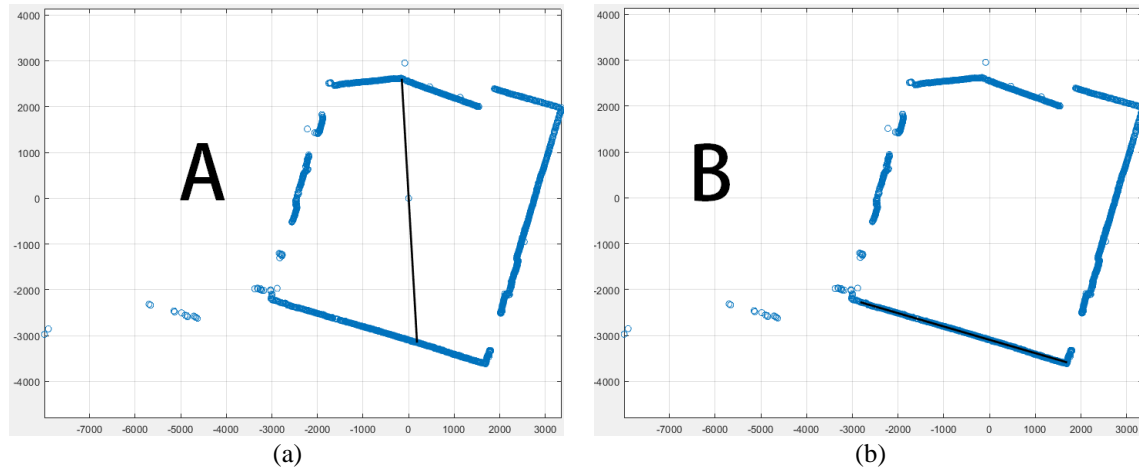


Figure 7. RANSAC method with ungrouped data. The x and y axes show the distance between detected points and LiDAR position in mm; (a) affects identification process for RANSAC's inlier and (b) RANSAC is able to identify the inlier

As shown in Figure 8, LiDAR data is classified into four major groups based on their location on the x- and y-axes. The first group is on the negative x and positive y axes, the second group is on the positive x and positive y axes, the third group is on the negative x and y axes, and the fourth group is on the positive x and negative y axes. In addition, the methods are used to determine whether grouped data is still necessary. The methods used in the first, third, and fourth groups are shown in Figure 9. The inlier is clearly identified after implementation, but the line-fitting position remains insufficient. To address this issue, data is then divided into smaller groups. The second group is not required, since the gaps between the data are not parallel as shown in Figure 10. These gaps are caused by objects blocking the walls rather than data loss. If the method is used, it has the potential to change the dimensions of a room, as illustrated in Figures 11(a) and (b). The derived results concluded that the RANSAC method used in this experiment is ineffective when applied to a room with many objects blocking the walls.

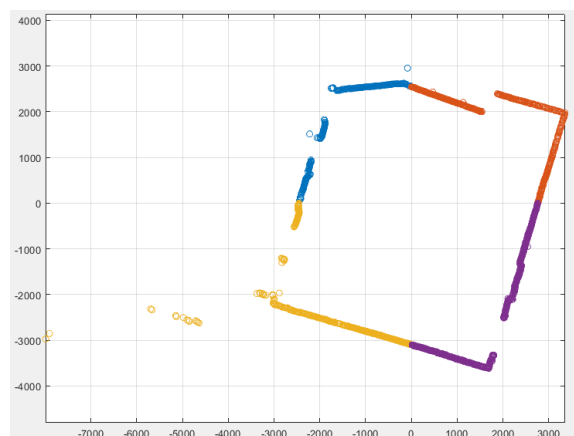


Figure 8. Visualization of LiDAR data after data grouping. The x and y axes show the distance between detected points and LiDAR position in mm

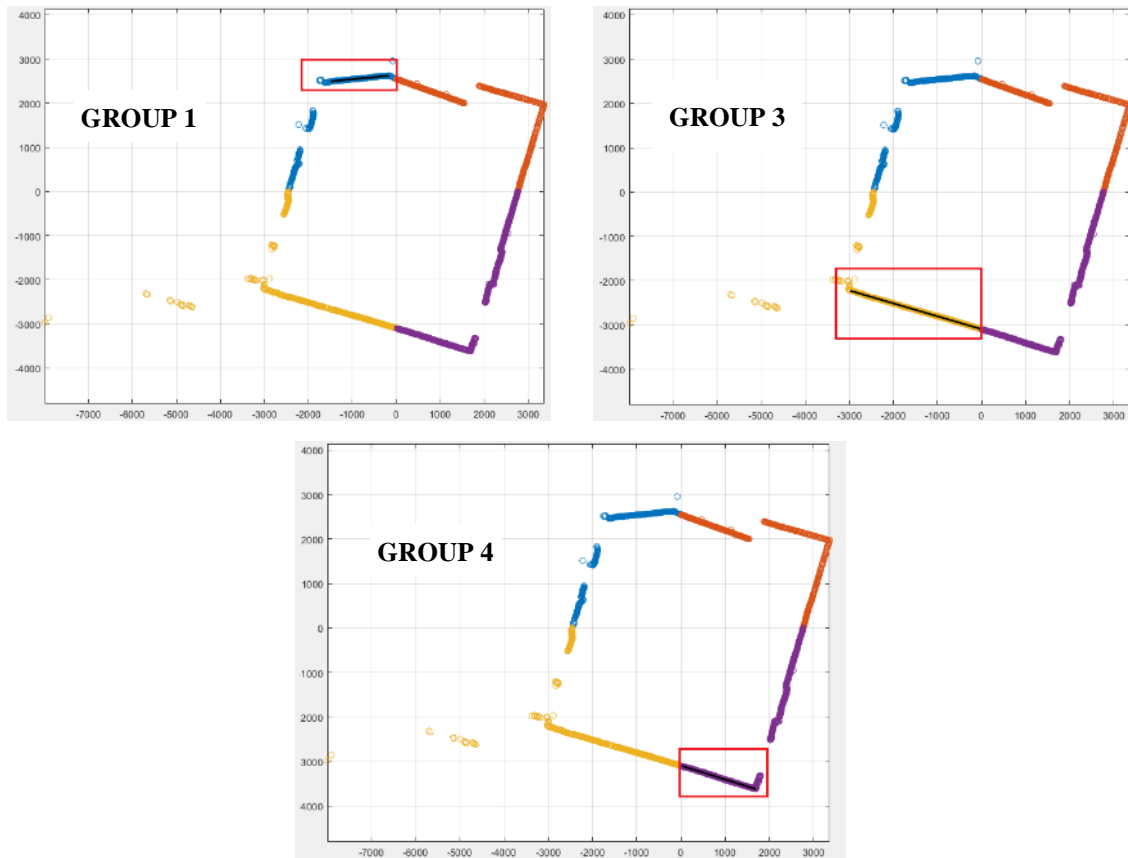


Figure 9. The groups 1, 2, and 3 with implementation of RANSAC method. The x and y axes show the distance between detected points and LiDAR position in mm

The RANSAC method is able to generate multiple models. However, if only one model is matched, the results in some cases is similar. The best model is then selected from among these based on a number of parameters, such as the model with the most outliers (undeveloped RANSAC method).

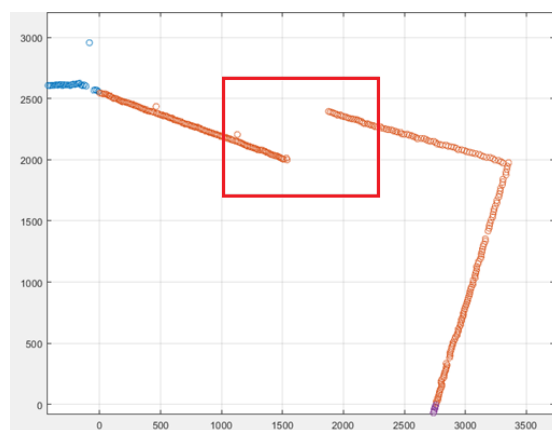


Figure 10. Data gap in group 2. The x and y axes show the distance between detected points and LiDAR position in mm

To achieve satisfactory results, the first data group requires two sub-groups with one line-fitting, the third data group requires ten sub-groups with two line-fittings, and the fourth data group requires six sub-groups with one line-fitting. The first group results six models as shown in Figure 12 (in Appendix). In the third group,

the method is applied twice. The first implementation results the two models as shown in Figure 13. The second implementation results one model as shown in Figure 14. Implementation in the fourth group results two models as shown in Figures 15(a) and (b). The RANSAC method is implemented to each group.

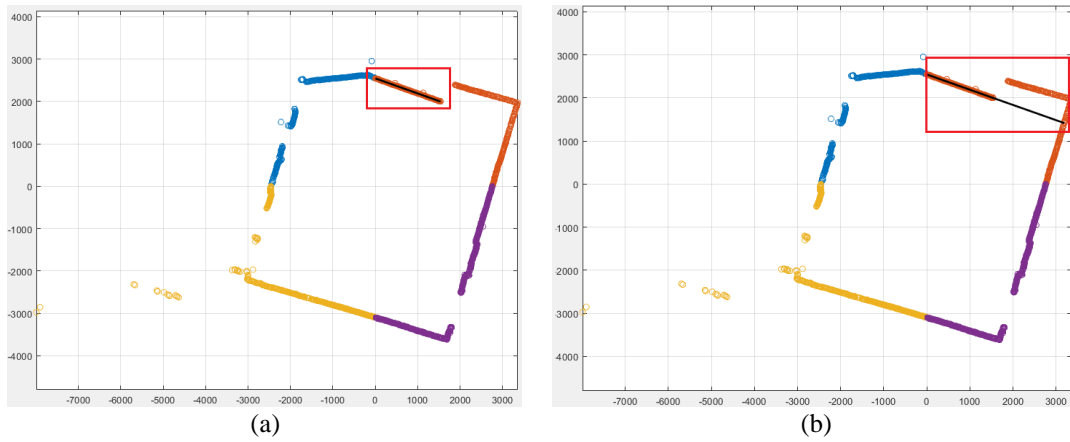


Figure 11. RANSAC method implementation in group 2. The x and y axes show the distance between detected points and LiDAR position in mm; (a) only one group involved (b) two groups are involved

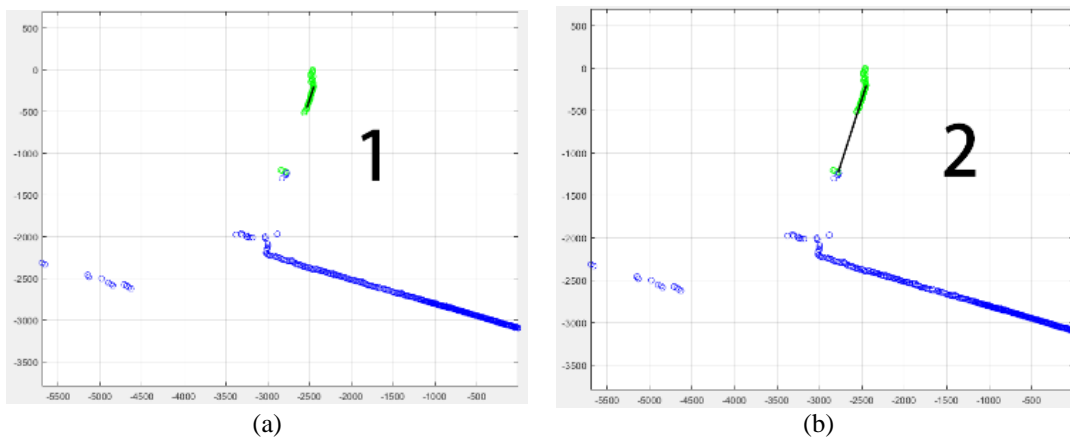


Figure 13. Implementation of undeveloped RANSAC method (group 3a). The x and y axes show the distance between detected points and LiDAR position in mm; (a) the first model and (b) the second model

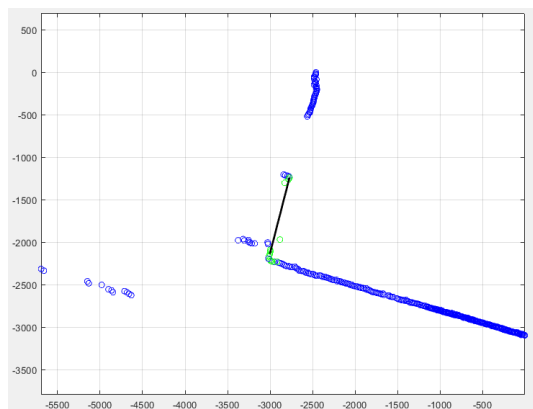


Figure 14. Implementation of undeveloped RANSAC method (group 3b). The x and y axes show the distance between detected points and LiDAR position in mm

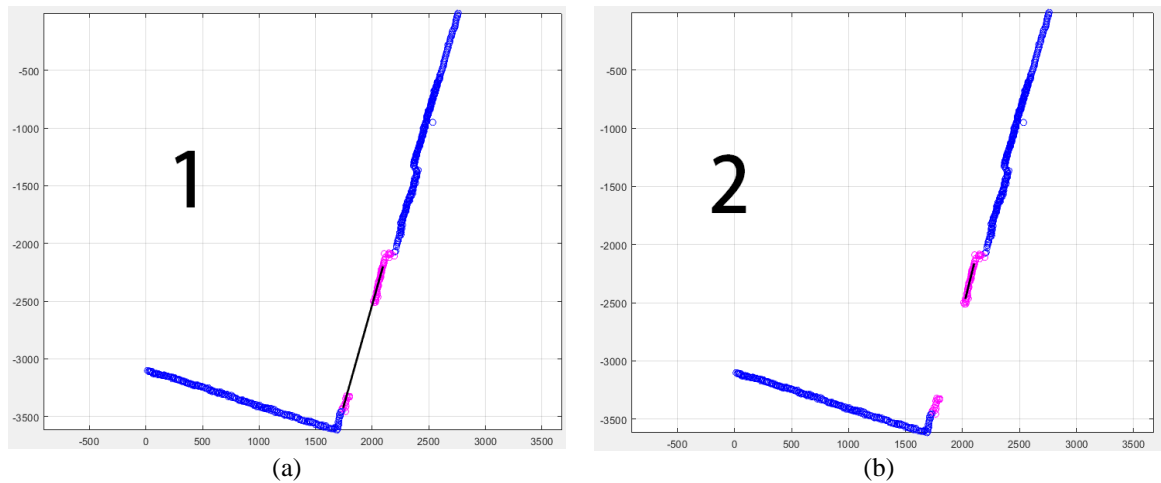


Figure 15. Implementation of undeveloped RANSAC method (group 4). The x and y axes show the distance between detected points and LiDAR position in mm; (a) the first model and (b) the second model

There are several data groups that have more than one RANSAC model based on the results of using the undeveloped method. One method for selecting the best model is to consider the number of outliers. The model with the greatest number of inliers must be selected. However, this experiment proposes selecting a model based on the maximum distance parameter between the x and y points that form the line (developed RANSAC method). The experiment executes 10, 100, and 1,000 times. The RANSAC method has a maximum default number of iterations of 1,000. The RANSAC model's stability is proportional to the number of iterations.

The results with developed method are more stable. However, the processing time is longer than the use of undeveloped method. The use of undeveloped method requires the processing time for each group is approximately 8-10 seconds while developed method requires approximately 10-20 seconds for 10 iterations, 30-60 seconds for 100 iterations, and 640-1,200 seconds for 1,000 iterations. Figure 16 shows the results with developed method. The results of this experiment show that line-fitting to reconstruct lost data using the RANSAC method on a room map is possible. The RANSAC method's implementation is limited to reconstructing the edges of the room that are not readable during the scanning process. This method is unsuitable for reconstructing a room with numerous obstacles. The data processing time required for the undeveloped method is approximately 8-10 seconds, whereas the processing time with developed method is approximately 10-20 seconds for 10 iterations, 30-60 seconds for 100 iterations, and 640-1,200 seconds or approximately 10-20 minutes for 1,000 iterations for the entire group.

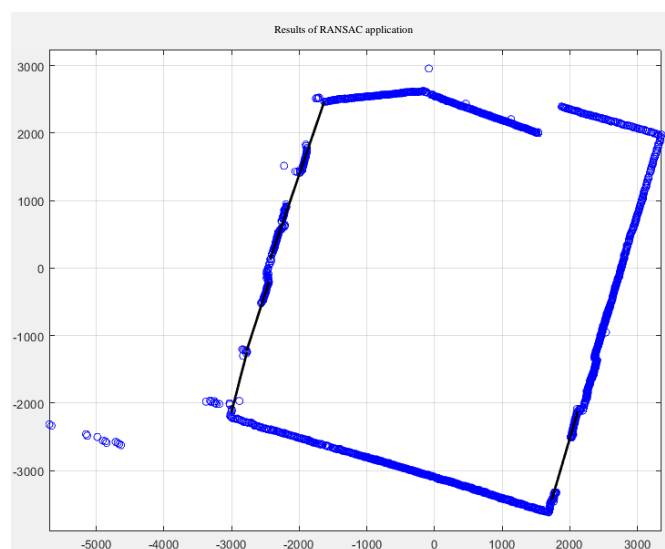


Figure 16. Implementation of developed RANSAC method. The x and y axes show the distance between detected points and LiDAR position in mm

Figure 17 shows a graph for the number of iterations against data processing time, with the horizontal axis representing the number of iterations and the vertical axis representing the data processing time in seconds. According to the graph, the number of iterations is directly proportional to the data processing time, which means that as the number of iterations increases, the data processing time required increases.

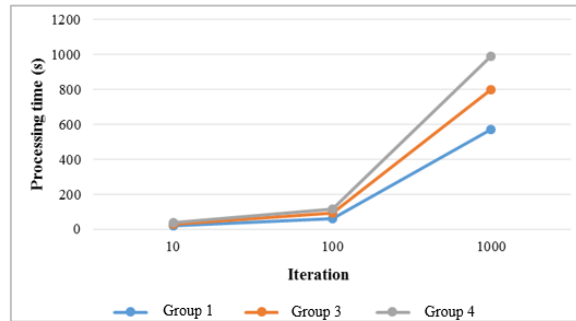


Figure 17. Processing time as a function of number of iteration

Furthermore, the best model in each group is selected based on the maximum distance. The distance data for each iteration (10, 100, and 1,000 times) for each group is formed as a graph for comparison in order to determine the maximum distance between x and y points. The horizontal axis represents the number of iterations, while the vertical axis is the x and y distance (mm). Figure 18 shows the distance data for group 1 after 10 iterations, Figure 19 shows the distance data after 100 iterations, and Figure 20 shows the distance data after 1,000 iterations. The distance graph shows a maximum distance of 1843.594413 mm for iterations of 10 times, and a maximum distance of 2468.192472 mm for iterations of 100 and 1,000 times. Based on these findings, it is concluded that the best model in Group 1 can be determined with between 100 and 1,000 iterations. Figures 21 to 23 show the x-y distance graph for group 3 with 10 iterations, 100 iterations, and 1,000 iterations, respectively. The maximum x-y distance for iterations of 10, 100, or 1,000 times in group 3a and 3b are 1073.965074 mm and 926.6370847 mm, respectively.

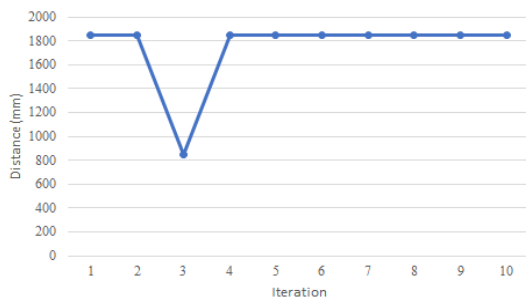


Figure 18. x-y distance with 10 iterations for group 1

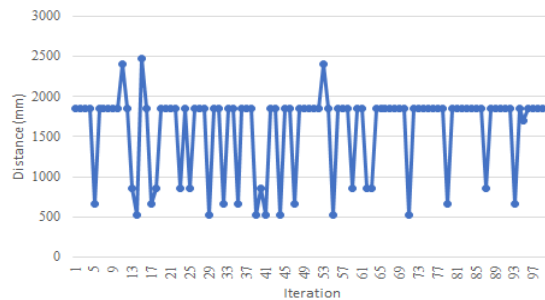


Figure 19. x-y distance with 100 iterations for group 1

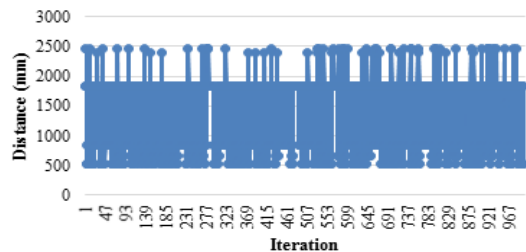


Figure 20. The x-y distance with 1,000 iterations for group 1

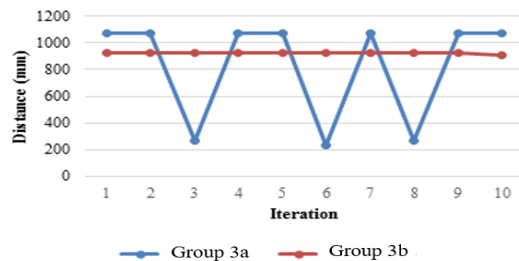


Figure 21. The x-y distance with 10 iterations for group 3

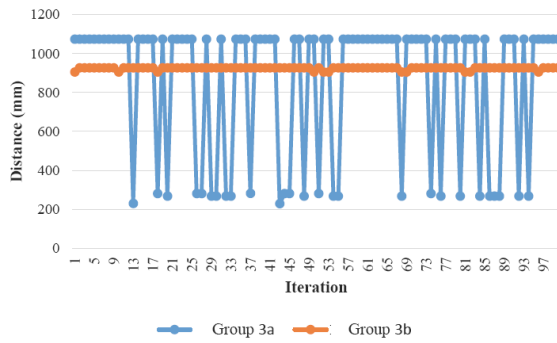


Figure 22. The x-y distance with 100 iterations for group 3

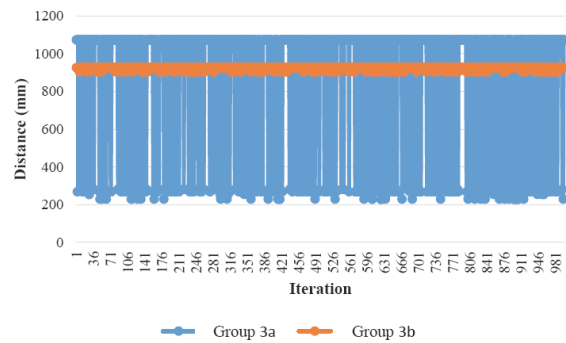


Figure 23. The x-y distance with 1,000 iterations for group 3

Figures 24 to 26 show the x-y distance graph for group 4 with 10 iterations, 100 iterations, and 1,000 iterations, respectively. The maximum distance in group 4 is 1379.93938 mm for 10 iterations, and 1380.827009 mm for 100 and 1,000 iterations. According to the results, the x-y distance with 10 iterations results unstable model. The model is more stable when iterations are performed more frequently, but it needs more processing time. Furthermore, the room map visualization is improved after implementing the RANSAC method with higher iteration process.

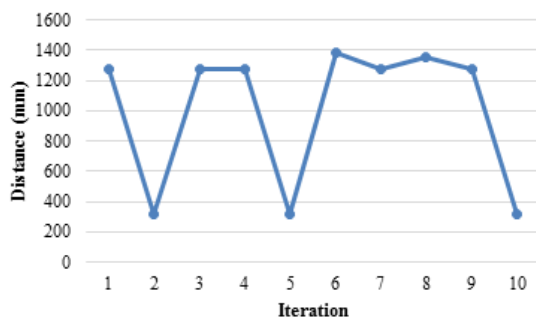


Figure 24. The x-y distance with 10 iterations for group 4

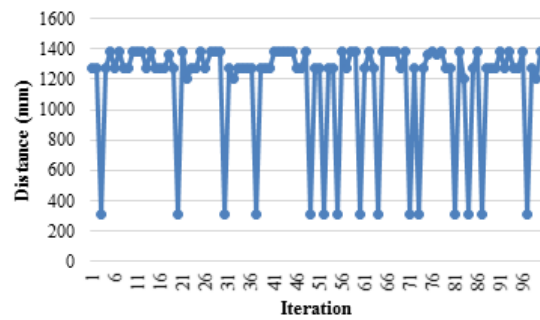


Figure 25. The x-y distance with 100 iterations for group 4

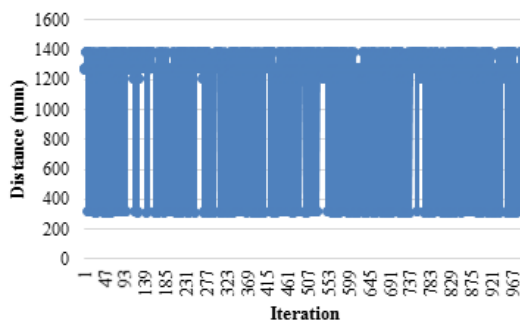


Figure 26. x-y distance t with 1,000 iterations for group 4

4. CONCLUSION

Room mapping with LiDAR has been studied. The adoption of the RANSAC approach for line-fitting is considered a solution to the problem of missing or illegible LiDAR point cloud data during the scanning process owing to reflection or impediments. The number of data used has an impact on the number of RANSAC models produced. The likelihood that there will be more appropriate models increases in direct proportion to the volume of data used. Additionally, the RANSAC method permits the random selection of

sample points for many models, hence altering the obtained findings. One option for choosing an appropriate model in room mapping is the established RANSAC approach, which is a suggested strategy for determining the maximum x-y distance. Moreover, the required model may be obtained by increasing the number of repetitions. But the processing time goes up. With 100 and 1,000 iterations, the greatest x-y distance can be found.

APPENDIX

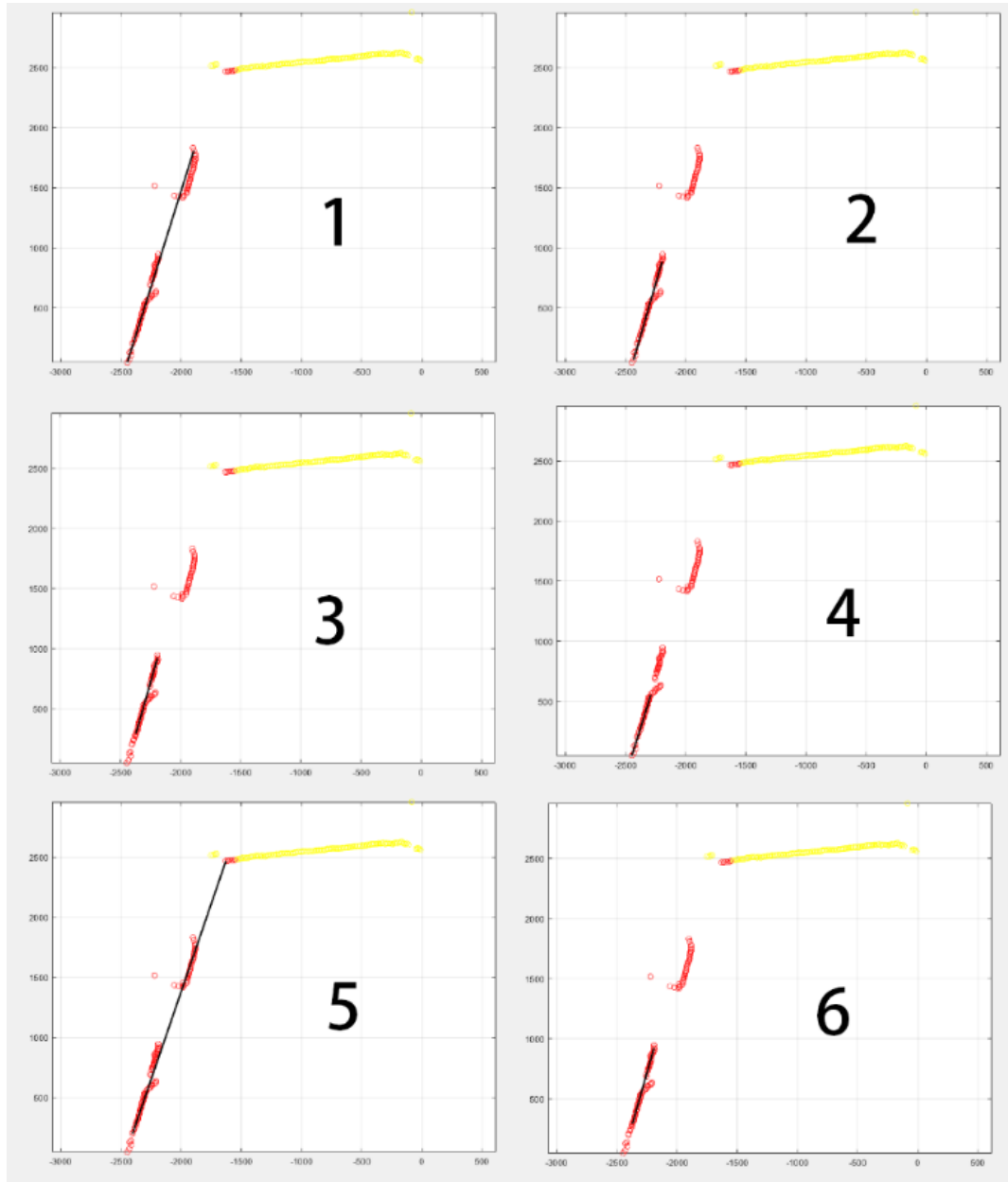


Figure 12. Implementation of undeveloped RANSAC method (group 1). The x and y axes show the distance between detected points and LiDAR position in mm

ACKNOWLEDGEMENTS

Special credit is addressed to the Indonesia Endowment Fund for Education, which had support fund for this research through the Riset dan Inovasi untuk Indonesia Maju (RIIM) program, organized by the National Research and Innovation Agency (BRIN).

REFERENCES

- [1] F. Hosoi, Y. Nakai, and K. Omasa, "Estimation and error analysis of woody canopy leaf area density profiles using 3-D airborne and ground-based scanning lidar remote-sensing techniques," *IEEE Transactions on Geoscience and Remote Sensing*, vol. 48, no. 5, pp. 2215-2223, May 2010, doi: 10.1109/TGRS.2009.2038372.
- [2] S. Xia and R. Wang, "Façade separation in ground-based LiDAR point clouds based on edges and windows," *IEEE Journal of Selected Topics in Applied Earth Observations and Remote Sensing*, vol. 12, no. 3, pp. 1041-1052, March 2019, doi: 10.1109/JSTARS.2019.2897987.
- [3] H. Liu *et al.*, "Deep learning in forest structural parameter estimation using airborne LiDAR data," *IEEE Journal of Selected Topics in Applied Earth Observations and Remote Sensing*, vol. 14, pp. 1603-1618, 2021, doi: 10.1109/JSTARS.2020.3046053.
- [4] B. Li, "On enhancing ground surface detection from sparse lidar point cloud," *IEEE/RSJ International Conference on Intelligent Robots and Systems (IROS)*, 2019, pp. 4524-4529, doi: 10.1109/IROS40897.2019.8968135
- [5] C. Wang *et al.*, "Evaluation of footprint horizontal geolocation accuracy of spaceborne full-waveform LiDAR based on digital surface model," *IEEE Journal of Selected Topics in Applied Earth Observations and Remote Sensing*, vol. 13, pp. 2135-2144, 2020, doi: 10.1109/JSTARS.2020.2992094.
- [6] S. Matteoli, M. Diani, and G. Corsini, "ARTEMIdE—an automated underwater material recognition method for fluorescence LIDAR invariant to environmental conditions," *IEEE Transactions on Geoscience and Remote Sensing*, vol. 58, no. 3, pp. 1763-1776, March 2020, doi: 10.1109/TGRS.2019.2948428.
- [7] J. C. F. Diaz, W. E. Carter, R. L. Shrestha, and C. L. Glennie, *LiDAR Remote Sensing*, Handbook of Satellite Applications Second Edition-Volume 2, Swiss, Springer International Publishing, 2017, p. 930.
- [8] F. Tarsha-Kurdi, T. Landes, and P. Grussenmeyer, "Hough-transform and extended RANSAC Algorithms for automatic detection of 3D building roof planes from lidar data," *ISPRS Workshop on Laser Scanning*, 2007.
- [9] M. Fan, S. -W. Jung, and S. -J. Ko, "Highly accurate scale estimation from multiple keyframes using RANSAC plane fitting with a novel scoring method," *IEEE Transactions on Vehicular Technology*, vol. 69, no. 12, pp. 15335-15345, Dec. 2020, doi: 10.1109/TVT.2020.3040014.
- [10] B. Li, D. Ming, W. Yan, X. Sun, T. Tian, and J. Tian, "Image matching based on two-column histogram hashing and improved RANSAC," *IEEE Geoscience and Remote Sensing Letters*, vol. 11, no. 8, pp. 1433-1437, Aug. 2014, doi: 10.1109/LGRS.2013.2295115.
- [11] A. P. D. Poz and M. S. Yano, "Ransac-based segmentation for building roof face detection in lidar point cloud," In *Proc. IGARSS - 2018 IEEE International Geoscience and Remote Sensing Symposium*, 2018, pp. 1276-1279, doi: 10.1109/IGARSS.2018.8518502.
- [12] P. C. Niedfeldt, K. Ingersoll, and R. W. Beard, "Comparison and analysis of recursive-RANSAC for multiple target tracking," *IEEE Transactions on Aerospace and Electronic Systems*, vol. 53, no. 1, pp. 461-476, Feb. 2017, doi: 10.1109/TAES.2017.2650818.
- [13] Y. Budisusanto, M. N. Cahyadi, I. W. Farid, M. R. Ubaidillah, and D. W. Imani, "Low cost LiDAR prototype design for 3D mapping," in *2021 International Conference on Advanced Mechatronics, Intelligent Manufacture and Industrial Automation (ICAMIMIA)*, Surabaya, Indonesia, 2021, pp. 13-17, doi: 10.1109/ICAMIMIA54022.2021.9808695.
- [14] J. Li and R. Stevenson, "2D LiDAR and camera fusion using motion cues for indoor layout estimation," in *2021 IEEE 24th International Conference on Information Fusion (FUSION)*, Sun City, South Africa, 2021, pp. 1-6, doi: 10.23919/FUSION49465.2021.9627040.
- [15] V. M. Chainago, A. N. Jati, and C. Setianingsih, "Development of non-platform mobile robot for simultaneous localization and mapping using ROS," in *2019 IEEE International Conference on Aerospace Electronics and Remote Sensing Technology (ICARES)*, Yogyakarta, Indonesia, 2019, pp. 1-6, doi: 10.1109/ICARES.2019.8914356.
- [16] T. H. Chan, H. Hesse, and S. G. Ho, "LiDAR-based 3D SLAM for indoor mapping," in *2021 7th International Conference on Control, Automation and Robotics (ICCAR)*, Singapore, 2021, pp. 285-289, doi: 10.1109/ICCAR52225.2021.9463503.
- [17] V. -I. Ungureanu, B. -A. Trutiu, I. Silea, P. Negirla, C. Zimbru, and R. -C. Miclea, "Automatic mapping of a room using LIDAR-based measuring sensor," in *2019 22nd International Conference on Control Systems and Computer Science (CSCS)*, Bucharest, Romania, 2019, pp. 689-695, doi: 10.1109/CSCS.2019.00123.
- [18] H. Yoshisada, Y. Yamada, A. Hiromori, H. Yamaguchi, and T. Higashino, "Indoor map generation from multiple LIDAR point clouds," in *2018 IEEE International Conference on Smart Computing (SMARTCOMP)*, Taormina, Italy, 2018, pp. 73-80, doi: 10.1109/SMARTCOMP.2018.00076.
- [19] P. Alliez *et al.*, "Real-time multi-SLAM system for agent localization and 3D mapping in dynamic scenarios," in *2020 IEEE/RSJ International Conference on Intelligent Robots and Systems (IROS)*, Las Vegas, NV, USA, 2020, pp. 4894-4900, doi: 10.1109/IROS45743.2020.9340646.
- [20] M. Tabata, Y. Takeuchi, Y. Yao, R. Tanaka, and J. Tamamatsu, "3D mapping for panoramic inspection images to improve manhole diagnosis efficiency," in *2022 IEEE/SICE International Symposium on System Integration (SII)*, Narvik, Norway, 2022, pp. 590-595, doi: 10.1109/SII52469.2022.9708903.
- [21] L. Charlemagne, G. David, and A. H. Ballado, "Mapping mangrove forest from LiDAR data using object-based image analysis and Support Vector Machine: The case of Calatagan, Batangas," *2015 International Conference on Humanoid, Nanotechnology, Information Technology, Communication and Control, Environment and Management (HNICEM)*, Cebu, Philippines, 2015, pp. 1-5, doi: 10.1109/HNICEM.2015.7393167.
- [22] Z. Shao, L. Zhang, and L. Wang, "Stacked sparse autoencoder modeling using the synergy of airborne LiDAR and satellite optical and SAR data to map forest above-ground biomass," *IEEE Journal of Selected Topics in Applied Earth Observations and Remote Sensing*, vol. 10, no. 12, pp. 5569-5582, Dec. 2017, doi: 10.1109/JSTARS.2017.2748341.
- [23] N. Baras, G. Nantzios, D. Ziouzos and M. Dasygenis, "Autonomous Obstacle Avoidance Vehicle Using LIDAR and an Embedded System," *2019 8th International Conference on Modern Circuits and Systems Technologies (MOCAST)*, Thessaloniki, Greece, 2019, pp. 1-4, doi: 10.1109/MOCAST.2019.8742065.
- [24] M. Yoshioka, N. Suganuma, K. Yoneda and M. Aldibaja, "Real-time object classification for autonomous vehicle using LIDAR," *2017 International Conference on Intelligent Informatics and Biomedical Sciences (ICIIBMS)*, Okinawa, Japan, 2017, pp. 210-211, doi: 10.1109/ICIIBMS.2017.8279696.
- [25] T. Kim and T. Park, "Placement optimization of multiple lidar sensors for autonomous vehicles," *IEEE Transactions on Intelligent Transportation Systems*, vol. 21, no. 5, pp. 2139-2145, May 2020, doi: 10.1109/TITS.2019.2915087.
- [26] P. Sun, X. Zhao, Z. Xu, R. Wang, and H. Min, "A 3D LiDAR data-based dedicated road boundary detection algorithm for autonomous vehicles," *IEEE Access*, vol. 7, pp. 29623-29638, 2019, doi: 10.1109/ACCESS.2019.2902170.
- [27] R. Changalvala and H. Malik, "LiDAR data integrity verification for autonomous vehicle," *IEEE Access*, vol. 7, pp. 138018-




- 138031, 2019, doi: 10.1109/ACCESS.2019.2943207.
- [28] A. Rangesh and M. M. Trivedi, "No blind spots: full-surround multi-object tracking for autonomous vehicles using cameras and LiDARs," *IEEE Transactions on Intelligent Vehicles*, vol. 4, no. 4, pp. 588-599, Dec. 2019, doi: 10.1109/TIV.2019.2938110.
- [29] X. Wang, Y. Cai, and T. Shi, "Road edge detection based on improved RANSAC and 2D LIDAR Data," 2015 International Conference on Control, Automation and Information Sciences (ICCAIS), Changshu, 2015, pp. 191-196, doi: 10.1109/ICCAIS.2015.7338660.
- [30] A. S. Satyawan, D. Kurniawan, N. Armi, and Y. N. Wijayanto, "Room map estimation from two-dimensional lidar's point cloud data, 2019 International Conference on Radar, Antenna, Microwave, Electronics, and Telecommunications (ICRAMET), Tangerang, Indonesia, 2019, pp. 152-155, doi: 10.1109/ICRAMET47453.2019.8980374.

BIOGRAPHIES OF AUTHORS






Merlyn Inova Christie Latukolan    received bachelor of engineering and master of engineering from School of Electrical Engineering, Telkom University in 2020 and 2022, respectively. During her studies, she worked as a research assistant at Nanosatellite Laboratory and was a recipient of the Telkom University Digital Talent Scholarship 2021. She was also an internship student in PT. Telekomunikasi Indonesia. Currently, she is working for a satellite telecommunication company which focuses on management and regulation. She can be contacted at email: christieltkln46@gmail.com.






Aloysius Adya Pramudita    received the B.S. degree in electrical engineering from Gadjah Mada University, Indonesia, in 2000, and the M.S. and Ph.D. degrees in electrical engineering from the Bandung Institute of Technology, Indonesia, in 2005 and 2009, respectively. From 2002 to 2016, he was a Lecturer and a Researcher with Atma Jaya Catholic University, Indonesia, where he was the Head of the Department of Electrical Engineering, from 2013 to 2016, and the Head of the Electrical Engineering Graduate Program, from 2016 to 2017. Since 2017, he has been with the Department of Telecommunication Engineering, Telkom University, Bandung, Indonesia. Since 2020, he has been the Director of the Internet of Things Research Center, Telkom University, that focuses on intelligent sensing research area. He is currently a member of the Telkom University Radar Research Group. He is also the Head of the Satellite Communication and Radar Laboratory, Telkom University. His research interests include antenna theory and design for telecommunication and radar, electromagnetics and wave application, and radar system for contactless sensor. He serves as a reviewer for several technical journals and conferences in his interest area. He can be contacted at email: pramuditaadya@telkomuniversity.ac.id.






Nasrullah Armi    received master of engineering degree from Department of Knowledge based Information Engineering, Toyohashi University of Technology, Japan in 2004. Subsequently, he obtained his Ph.D. degree from Department of Electrical and Electronic Engineering, Universiti Teknologi Petronas, Malaysia in 2013. His research interests are signal processing, wireless communication and networks. He published scientific articles on peer review journals and participated in international conferences. He contributed his knowledge as scientific reviewer in international impact journals and became Scientific Committee in International Conferences. Currently, he is working as a researcher at the National Research and Innovation Agency, Research Center for Telecommunication. He can be contacted at email: nasrullah.armi@gmail.com.



Nizar Alam Hamdani    received a doctorate in management and education at the Indonesian University of Education, completing a master's program at the Bandung Institute of Technology and Telkom University. He has published research in management, information technology, and educational technology. He has various experiences as a consultant in Economics and Information Technology and as an entrepreneur. He can be contacted at email: nizar_hamdani@uniga.ac.id.



Helfy Susilawati    received bachelor's degree in physical education in 2011 from UIN Sunan Gunung Djati Bandung, Bandung, Indonesia, and a master's degree in electrical engineering in 2014 from Institut Teknologi Bandung (ITB) in Bandung, Indonesia. She has worked as a lecturer at Universitas Garut, Indonesia, since 2012. Her research interest includes a control system, image processing, and artificial intelligence. She can be contacted at email: helfy.susilawati@uniga.ac.id.



Arief Suryadi Satyawan    received his bachelor's degree in electrical engineering from Universitas Jenderal Achmad Yani Bandung, Indonesia, in 2000. In 2007, he received his Master's degree in electrical engineering from Institut Teknologi Bandung, Indonesia. He obtained his Ph.D. in computer and communication engineering from Waseda University, Japan, in 2019. His current research is image and video processing, and video communication systems. He is a member of The Institute of Image Information and Television Engineers (ITE), Japan, and Information Processing Society of Japan (IPSJ). Currently, he is working as a researcher at the National Research and Innovation Agency, Research Center for Telecommunication. He can be contacted at email: arie021@brin.go.id.